Available online at www.sciencedirect.com
SCIENCE DIRECT®
Pergamon
Cement and Concrete Research 34 (2004) 1481–1488
CEMENT AND CONCRETE RESEARCH

The crystal structure of jennite, $Ca_9Si_6O_{18}(OH)_6{\cdot}8H_2O$

E. Bonaccorsi*, S. Merlino, H.F.W. Taylor [1]

Dipartimento di Scienze della Terra, Via S. Maria 53, I-56126 Pisa, Italy

Received 3 October 2003; accepted 29 December 2003

Abstract

The crystal structure of jennite is solved and refined in the space group $P\bar{1}$, by using single crystal X-ray diffraction data collected at the Elettra synchrotron radiation facility on a very thin crystal from Fuka, Japan. The triclinic refined unit cell is $a = 10.576(2)$ Å, $b = 7.265(2)$ Å, $c = 10.931(3)$ Å, $\alpha = 101.30(1)$, $\beta = 96.98(1)$, $\gamma = 109.65(1)°$. The structure of jennite is built up by three distinct modules: ribbons of edge-sharing calcium octahedra, silicate chains of wollastonite-type running along **b**, and additional calcium octahedra on inversion centres. The structural results indicate that the crystal chemical formula of jennite is $Ca_9Si_6O_{18}(OH)_6{\cdot}8H_2O$, and that all the hydroxyl groups are bonded to three calcium cations; SiOH groups are not found. The structural disorder observed in jennite is explained on the basis of the OD theory, and a model for the structure of metajennite, the dehydration product of jennite, is proposed.

Keywords: Jennite; Calcium–silicate–hydrate, (C–S–H); Crystal structure; X-ray diffraction; Portland cement

1. Introduction

Jennite is a rare mineral, firstly found at Crestmore, CA [1,2] and, later, in Israel [3], Germany [4,5], Italy [6], Japan; [7], South Africa [8], and Jordan [9]. It has been also synthesised hydrothermally (from CaO and fumed silica [10], and from CaO and acid silica [11]). Its importance lies mainly in its possible relationships with C–S–H, the poorly crystalline material, which forms during the hydration of Portland cement. In fact, several data indicate that both tobermorite- and jennite-like domains occur in C–S–H, and that over a period of months and years, the jennite-type structures become increasingly dominant [12]. Recent results [13] relate different solubility curves of C–S–H to its different nanostructures, which range from a purely tobermorite-like to a largely jennite-like structure. However, no structural refinement of jennite was hitherto available, so that its relationships with the nanostructure of C–S–H are largely conjectured.

The aim of this work is to present the structural results we obtained from single-crystal data on a specimen of natural jennite, to clarify its structural arrangement and to give a sound basis for future works on C–S–H nanostructures.

2. Previous results

The chemical composition reported in the original description of jennite [1] has been refined by successive chemical analyses [2,7], which pointed to the chemical formula $Ca_9(Si_6O_{18}H_2)(OH)_8{\cdot}6H_2O$. The X-ray diffraction pattern of jennite is characterised by weak reflections with odd values of k. By neglecting these reflections, an A-centred monoclinic pseudocell is obtained with $a = 9.947(6)$ Å, $b = 3.642(3)$ Å, $c = 21.37\ (1)$ Å, $\beta = 101.90(7)°$ [2]. The true cell is triclinic, $a = 10.593$ Å, $b = 7.284$ Å, $c = 10.839$ Å, $\alpha = 99.67°$, $\beta = 97.65°$, $\gamma = 110.11°$, and it can be obtained from the pseudocell by applying the transformation matrix given in Table 1. The odd k reflections may be sharp or give streaks parallel to **a*** of the pseudocell, so indicating that disorder can occur in that direction. A TEM study [14] on a disordered synthetic sample of jennite suggests that "the origin of the streaking is due to the stacking of the layers with various periodicities along the [100]", resulting from the shift of **b**/2 of the tetrahedral chains, possibly related to the observed fluctuations of the local Ca/Si ratio.

If jennite is heated in air at 70–90 °C, molecules of water are lost, and the unit cell shrinks in the **c** direction; the d value of the strong 002 reflection (indices referred to the monoclinic pseudocell) decreases from 10.45 to 8.69 Å. The dehydration product is named metajennite [1]. Metajennite presents the diffraction features just described for jennite,

* Corresponding author. Tel.: +39-050-847-204; fax: +39-050-40976.
E-mail address: elena@dst.unipi.it (E. Bonaccorsi).
[1] Deceased as of November 25, 2002.

0008-8846/$ – see front matter © 2004 Elsevier Ltd. All rights reserved.
doi:10.1016/j.cemconres.2003.12.033

Table 1
Parameters (in Å and degrees) of the pseudocells and true cells of jennite and metajennite, taken from Ref. [2]

	Jennite	Metajennite	Transformation matrices
A-centred pseudocell	$a=9.947$ $b=3.642$ $c=21.37$ $\beta=101.90$	$a=9.945$ $b=3.639$ $c=18.67$ $\beta=111.44$	*A*-centred to *I*-centred pseudocell: [Ī, 0, 0 / 0, Ī, 0 / 1, 0, 1] *A*-centred to true cell: [1, Ī, 0 / 0, 2, 0 / 0, $\overline{1/2}$, 1/2]
I-centred pseudocell	$a=9.947$ $b=3.642$ $c=21.63$ $\beta=104.84$	$a=9.945$ $b=3.639$ $c=17.656$ $\beta=100.18$	*I*-centred to *A*-centred pseudocell: [Ī, 0, 0 / 0, Ī, 0 / 1, 0, 1] *I*-centred to true cell: [Ī, 1, 0 / 0, 2̄, 0 / 1/2, 1/2, 1/2]
True cell	$a=10.593$ $b=7.284$ $c=10.839$ $\alpha=99.67$ $\beta=97.65$ $\gamma=110.11$	$a=10.590$ $b=7.278$ $c=9.511$ $\alpha=101.03$ $\beta=105.74$ $\gamma=110.10$	True cell to *A*-centred pseudocell: [1, 1/2, 0 / 0, 1/2, 0 / 0, 1/2, 2] True cell to *I*-centred pseudocell: [Ī, $\overline{1/2}$, 0 / 0, $\overline{1/2}$, 0 / 1, 1, 2]

with a distinction between the weak and sometimes diffuse reflections for odd k values and the strong reflections for even k values, corresponding, as in the case of jennite, to a monoclinic pseudocell. Table 1 presents the crystallographic data for both jennite and metajennite: the true unit cells, the pseudocells (beside the *A*-centred cell, also an *I*-centred pseudocell has been used by the previous authors), together with the corresponding transformation matrices.

A detailed discussion of the nature of the structural disorder occurring in both jennite and metajennite will be presented in a following paragraph.

Some data on the structure of jennite are available from spectroscopic studies. The occurrence of single chains (*dreierketten*) in jennite is confirmed by a ^{29}Si–NMR spectrum [15], in which the main peak, at −85.7 ppm, points to the occurrence of prevalent Q^2 sites. The presence of a consistent fraction of Q^1 sites, suggested in Ref. [15], is ruled out by the NMR study of Cong and Kirkpatrick [11], who found essentially Q^2 sites only and a few Q^1 sites, as chain-end tetrahedra, due to missing bridging tetrahedra. The ^{1}H–^{29}Si CPMAS NMR results [11] indicate that the Q^2 sites are indeed differentiated in two groups, as the Q^2 peak in the MAS spectrum is resolved into two narrow peaks, at −85.3 and −82.7 ppm. Moreover, the authors state that silicon atoms and at least some protons are strongly coupled in jennite, different from the other crystalline hydrated calcium silicate phases described in the same paper (tobermorites, xonotlite, hillebrandite, calciochondrodite). The ^{17}O MAS NMR spectrum of jennite [11] is similar with that of 1.4 nm tobermorite, except for some interesting features: (i) the different positions and intensities of the peaks attributed to nonbridging oxygen (NBO) atoms; (ii) the peak near 0 ppm, related to the water content, is narrower than the corresponding peak in 1.4 nm tobermorite; and (iii) the relative intensities of the peaks attributed to Ca–OH and Si–OH, respectively.

The same conclusions about the topology of the silicate chains in jennite are obtained through Raman [16] and infrared [17] spectroscopic studies.

3. The building of the starting model

The wide amount of data collected on the natural and synthetic samples of jennite, as well as some observed similarities with the 1.4 nm tobermorite structure, points to a model based on layers in which a central Ca–O corrugated sheet is flanked by rows of *dreierketten* and OH groups. The essential features of this model have been indicated by Taylor [18] many years ago, although it was impossible to completely assess the model and definitely test it with reliable diffraction data.

The Taylor model [18] had features in common with those of tilleyite and cuspidine, presenting the so-called tilleyite ribbons [19]. Those ribbons occur also in the structural arrangement of jaffeite [20,21], the natural analogue of the tricalcium silicate hydrate. A tilleyite ribbon is indicated in Fig. 1. In the figure, disilicate groups are connected to zigzag octahedral walls, forming infinite layers. A sound model for jennite has been built through different steps:

(a) First of all, additional ‘bridging’ tetrahedra are added to the disilicate groups to form *dreierketten*. The layers ($a=10.5$ Å, $b=7.3$ Å, $\gamma=110°$) are then stacked one after the other through the connection of the bridging tetrahedra of the layer, with apical oxygen atoms of the calcium octahedra of adjacent layers, to give rise to a structural arrangement with a triclinic cell $a=10.5$ Å, $b=7.3$ Å, $c=9.5$ Å, $\alpha=101$, $\beta=106$, $\gamma=110°$, closely corresponding to the unit cell of metajennite (see Fig. 5). Without any assumption about the relative position of the silicate chains, and assuming a disordered distribution of these chains in the structure, we obtained the set of coordinates for the average structure of metajennite, which gave rise to a calculated X-ray powder diffraction pattern, in acceptable agreement with the observed one.
(b) The set of coordinates corresponding to the true structure of metajennite in the triclinic cell may be derived from those of the average structure through the transformation

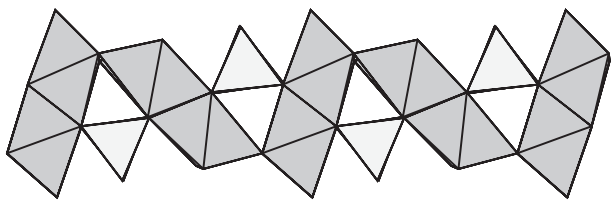

Fig. 1. A tilleyite ribbon. The Ca-occupied octahedra are indicated in dark grey, whereas the superimposed tetrahedra of the disilicate groups are coloured in light grey.

matrix given in Table 1, taking into due account that there are two possible relative positions of the silicate chains on both sides of the calcium octahedral walls.

(c) The final step is the passage from the true structure of metajennite to the true structure of jennite. The derivation is based on the obvious observation that the increase in the d_{001} distance from metajennite to jennite (8.69 and 10.46 Å, respectively) may be explained as due to the introduction of layers of water molecules (W), 1.77 Å wide, which alternate, in the jennite structure, with metajennite (MJ) layers (MJ–W–MJ–W–...). Through purely geometrical considerations, the relationships between the basis vectors in jennite and metajennite may be obtained ($\mathbf{a}_j = \mathbf{a}_{mj}$; $\mathbf{b}_j = \mathbf{b}_{mj}$; $\mathbf{c}_j = 0.191\ \mathbf{a}_{mj} + 0.146\ \mathbf{b}_{mj} + 1.202\ \mathbf{c}_{mj}$), and the model for jennite be built up.

4. Experimental

The natural samples of jennite we studied come from three different localities: (a) Crestmore, CA; (b) Zeilberg, Germany; (c) Fuka, Japan. All the samples are composed of nearly parallel or radial aggregates of thin fibres. Many of them were selected to collect single-crystal data by using synchrotron radiation at the Elettra facility (Trieste, Italy). The experiments were performed at the beamline 5.2 R (X-ray diffraction), the wavelength of the radiation was set to 0.99890 Å, and a 165-mm MarCCD detector was placed 50 mm from the sample. In this experimental setting, the irradiated sample is rotated about the φ axis by a few degrees, depending on its reciprocal spacings. Each recorded frame can be therefore used for the indexing process, refinement of the unit cell, and integration of the diffraction spots. The whole data collection can be finally obtained after the scaling of all the different frames.

However, all the trials to select single crystals from the Crestmore and Zeilberg samples failed, as the collected X-ray diffraction patterns indicated that they were always formed by many subparallel fibres, preventing any reliable indexing procedure and data collection. The same unlucky series of trials was repeated for the Fuka specimen, until an X-ray pattern was recorded, in which, together with the usual multifibre diffraction effects, a set of weak spots appeared due to a single crystal rotated nearly 60° with respect to the others. After carefully selecting these reflections, we used the Denzo [22] indexing program to find the following triclinic triacute cell: $a = 7.25$ Å, $b = 10.58$ Å, $c = 11.16$ Å, $\alpha = 74.2$, $\beta = 80.6$, $\gamma = 69.9°$. By applying the transformation matrix $|\bar{1}\ 1\ 0,\ 1\ 0\ 0,\ 0\ 0\ \bar{1}|$, the well-known unit cell of jennite was finally obtained and refined as $a = 10.576(2)$ Å, $b = 7.265(1)$ Å, $c = 10.931(2)$ Å, $\alpha = 101.34(1)$, $\beta = 96.98(1)$, $\gamma = 109.65(1)°$. Using the same crystal, 63 frames with $\Delta\varphi = 3°$ were collected; the frames were processed with the HKL package of programs [22]. A total of 2278 intensities ($-9 \le h \le 9$, $-6 \le k \le 5$, $-10 \le l \le 10$) was extracted from the 63 frames and corrected for background, Lorentz, and polarization factors. No absorption correction was performed.

5. Determination of the average structure

As the reflections with odd k were systematically very weak, we decided to use, initially, only the strong even k reflections to solve the average structure, which has a halved b parameter. This substructure was indeed solved in the space group $A2/m$, by using direct methods and successive Fourier maps (Shelx-97 package; [23]). The atoms, which were located by means of the direct methods, corresponded to the corrugated layer of CaO_6 octahedra, as predicted by the model, and to one interlayer calcium cation. Moreover, two symmetry-related silicon atoms were found in the position roughly corresponding to that of the paired tetrahedra of the silicate chain. The other atoms of the silicate chains were located through successive difference Fourier maps; they presented half occupancy and pointed to the simultaneous presence, in the average structure, of two chains shifted by **b**/2, with respect to each other. Finally, four symmetry-related electron density maxima, at distance of about 2.3 Å from the interlayer Ca cation, were attributed to water molecules. The least-square refinement of this average model converged to R=.16 by using only the 215 stronger reflections. This result confirmed the substantial correctness of the model and testified to the acceptable quality of the diffraction data, encouraging us to look for the real structure of jennite, using both even and odd k reflections.

6. Real structure refinement

The passage from the substructure to the real structure of jennite (the transformation matrix is reported in Table 1) implies an ordered arrangement of the silicate chains. The silicate chains, which are grasped on both sides of each octahedral ribbon, are displaced either by **b**/4 or $-$**b**/4. An ordered structure corresponding to the cell parameters of the triclinic true cell is realised when one of the two possible displacements is constantly applied (a more detailed discussion is presented in Section 7). The corresponding structural arrangement was successfully tested and refined in the space group $P\bar{1}$. The final refinement cycles, carried on by introducing anisotropic displacement parameters for the calcium cations of the walls and for the silicon cations, converged to R=.153 for 1278 reflections with $I > 4\sigma(I)$. Relevant data about the crystal and the intensity collection are reported in Table 2.

The final positional and displacement parameters are listed in Table 3, whereas selected bond distances are reported in Table 4.

Table 2
Crystal and structure refinement data for jennite

Empirical formula	$Ca_9Si_6O_{18}(OH)_6.8H_2O$
Formula weight	1063.44
Wavelength	0.99890 Å
Space group	$P\bar{1}$
Unit cell dimensions	$a=10.576(2)$ Å, $\alpha=101.30(1)^\circ$ $b=7.265(2)$ Å, $\beta=96.98(1)^\circ$ $c=10.931(3)$ Å, $\gamma=109.65(1)^\circ$
Z	1
Calculated density	2.325 g/cm^3
Absorption coefficient	1.912 mm^{-1}
Crystal size	Unknown
Theta range for data collection	3.58° to 28.45°
Limiting indices	$-9\le h\le 9$, $-6\le k\le 5$, $-10\le l\le 10$
Reflections collected/unique	2278/1950 [$R_{int}=0.1272$]
Completeness to $\theta=28.45$	88.1%
Refinement method	Full-matrix least-squares on F^2
Data/restraints/parameters	2278/0/130
$R=\frac{\sum \|\|F_o\|-\|F_c\|\|}{\sum \|F_o\|}$	0.153 for 1287 reflections with $I>4\sigma(I)$

6.1. Structure description

The crystal structure of jennite is reported in Fig. 2, in two different projections. It is built up by three distinct modules: ribbons of edge-sharing calcium octahedra, silicate chains of wollastonite-type (both ribbons and chains running along **b**), and additional calcium octahedra in special position on inversion centres. The ribbons—two octahedra large—are connected to each other by sharing vertices, giving rise to a zigzag layer of calcium octahedra, in which the ribbons are also firmly linked through the silicate chains running on both sides of it.

Two kinds of ribbon can be distinguished: in the former (Ca1, Ca3), all the vertices of the octahedra are shared with other polyhedra, namely, silicate tetrahedra and/or calcium octahedra, in the latter (Ca2, Ca4), the apices on both sides of the zigzag layer are free and correspond to water molecules.

The composite octahedral–tetrahedral (001) layers are connected through the additional calcium octahedra in special position.

6.2. Hydrogen bond system and chemical formula of jennite

The bond-valence sums for the various oxygen atoms of the structure were calculated according to the parameters listed in Ref. [24], and the corresponding values are reported in Table 5. Bond-valence sums largely different from 2 v.u. (valence units) were obtained for the atoms O8 (1.04 v.u.), O2 (1.09 v.u.), O11 (1.02 v.u.), and O12 (0.89 v.u.), besides for O13, O14, W1, and W2 (0.27, 0.21, 0.35 and 0.35 v.u., respectively), which certainly correspond to water molecules. The actual chemical nature of the former four atoms, i.e., if they are either hydroxyl groups or oxygen atoms, may be understood by looking at the complex system of hydrogen bonds connecting the H_2O molecules among them and to the oxygen atoms of the structure. A hydrogen bond system, which is in agreement with all the structural evidences, is drawn in Fig. 3. Here, we see that the atom O8, namely the free atom in the bridging tetrahedron, is the acceptor in three strong hydrogen bonds with the water molecules W1, W2, and O13. Applying the equation proposed in Ref. [25] to correlate bond valence versus O···O distance, an additional contribution of 0.92 v.u. to O8 may be calculated, indicating that O8 is actually an oxygen anion. On the other hand, the anions O2, O11, and O12 are hydroxyl groups. The bond valence sums, corrected by taking into account the hydrogen bonds system drawn in Fig. 3, are reported in the last column of Table 5. The formula of jennite, which results from the structure refinement, is therefore $Ca_9Si_6O_{18}(OH)_6.8H_2O$.

This crystal chemical formula refers to the natural sample we have studied, which shows a full occupancy of the interlayer Ca5 site. The occurrence of this calcium cation, which coordinates two hydroxyl groups and four water molecules at distances of 2.50 and 2.36 Å, respectively, results in the hydrogen bonding scheme reported in Fig. 3. However, it was observed [10–12] that, usually, the synthesised jennites show a C/S ratio lower than the ideal value of 1.5. In those samples, the deficit in positive charge is possibly balanced by a corresponding occurrence of OH^- groups in the O8 site, giving rise to the occurrence of Si–OH bonds. In fact, when Ca5 cations are absent, the water molecules are no more constrained to stay in the positions

Table 3
Fractional coordinates and isotropic displacement parameters U (Å^2) for jennite

	x	Y	z	U_{eq} or U_{iso}
Ca1	0.0601(5)	0.3632(9)	0.3648(6)	0.059(2)
Ca2	0.4226(5)	0.7984(9)	0.3617(6)	0.056(2)
Ca3	0.0658(6)	0.8664(9)	0.3769(6)	0.061(2)
Ca4	0.4289(6)	0.2954(9)	0.3531(6)	0.061(2)
Si1	0.8014(8)	0.942(1)	0.1939(8)	0.060(3)
Si2	0.7248(8)	0.241(1)	0.3748(8)	0.063(3)
Si3	0.7222(8)	0.673(1)	0.3784(8)	0.058(3)
O1	0.970(2)	0.024(3)	0.246(2)	0.051(5)
O2	0.273(2)	0.962(3)	0.308(2)	0.069(6)
O3	0.588(2)	0.129(3)	0.423(2)	0.047(5)
O4	0.872(2)	0.318(3)	0.487(2)	0.057(5)
O5	0.742(2)	0.121(3)	0.246(2)	0.068(6)
O6	0.720(2)	0.747(3)	0.249(2)	0.060(6)
O7	0.701(2)	0.433(3)	0.331(2)	0.071(6)
O8	0.756(2)	0.859(3)	0.0409(2)	0.047(5)
O9	0.581(2)	0.658(3)	0.429(2)	0.055(5)
O10	0.866(2)	0.794(3)	0.480(2)	0.058(6)
O11	0.273(2)	0.458(3)	0.303(2)	0.066(6)
O12	0.985(2)	0.542(3)	0.230(2)	0.065(6)
O13	0.443(2)	0.193(3)	0.129(2)	0.086(7)
O14	0.542(2)	0.191(3)	0.863(2)	0.080(7)
Ca5	0.0	0.5	0.0	0.072(3)
W1	0.914(2)	0.143(3)	0.941(2)	0.079(7)
W2	0.781(2)	0.519(3)	0.964(2)	0.083(7)

Table 4
Selected bond distances (Å) in jennite

Ca1	O1[a]	2.35(2)	Ca2	O3[b]	2.33(2)	Ca3[c]	O1	2.33(2)	Ca4	O2[d]	2.34(2)
	O11	2.35(2)		O9	2.35(2)		O2	2.33(2)		O9[b]	2.36(2)
	O12[c]	2.37(2)		O11	2.35(2)		O4[b]	2.36(2)		O11	2.40(2)
	O4[b]	2.38(2)		O3[e]	2.35(2)		O12[c]	2.39(2)		O13[f]	2.45(2)
	O10[b]	2.42(2)		O2	2.36(2)		O10[g]	2.46(2)		O9	2.48(2)
	O4b	2.49(2)		O14[b]	2.54(2)		O10[c]	2.47(2)		O3	2.51(2)
										O7	2.77(2)
Si1	O8	1.61(2)	Si2	O5	1.57(2)	Si3	O6	1.61(2)	Ca5	O12	2.50(2) × 2
	O6	1.65(2)		O3	1.61(2)		O10	1.62(2)		W1	2.36(2) × 2
	O5[e]	1.66(2)		O7	1.64(2)		O9	1.63(2)		W2	2.36(2) × 2
	O1	1.67(2)		O4	1.71(2)		O7	1.65(2)			

[a] $x+1, y, z$.
[b] $-x+1, -y+1, -z+1$.
[c] $x-1, y, z$.
[d] $x, y-1, z$.
[e] $x, y+1, z$.
[f] $x+1, y+1, z+1$.
[g] $-x+1, -y+2, -z+1$.

reported in Table 3, and the corresponding hydrogen bonds might not occur.

Several spectroscopic data suggest the occurrence of few SiOH groups in samples of synthetic jennite. In the room temperature ^{1}H MAS NMR spectrum [26], a small peak at 8 ppm was attributed to the hydrogen atoms belonging to SiOH groups, and the mid-IR spectrum of jennite shown in Ref. [17] displays a weak band at approximately 3740 cm^{-1}, attributed by the authors to SiO–H stretching in SiOH groups. On the other hand, the ^{1}H–^{29}Si CPMAS NMR results [11] evidenced a pronounced peak at −82.7 ppm, corresponding to one of the Q^2 sites (a bridging tetrahedron, according to our result), strongly coupled with at least some protons. The authors' conclusion [11] was that Si–OH linkages are present in jennite, but the observed strong interaction of the silicon and the protons could also depend on the occurrence of strong hydrogen bonds pointing to the free vertex of the bridging tetrahedron.

7. Disorder model

As we have previously said, jennite may display disorder in the sequence of the structural layers, as evidenced by diffuse reflections, or even continuous streaks, for odd k values, with diffuseness along **a*** [2,14]. These diffractional features, as well as the monoclinic symmetry displayed by the reflections with even k value, are characteristic of OD structures [27–30] consisting of equivalent layers. In such structures, neighbouring layers can be arranged in two or

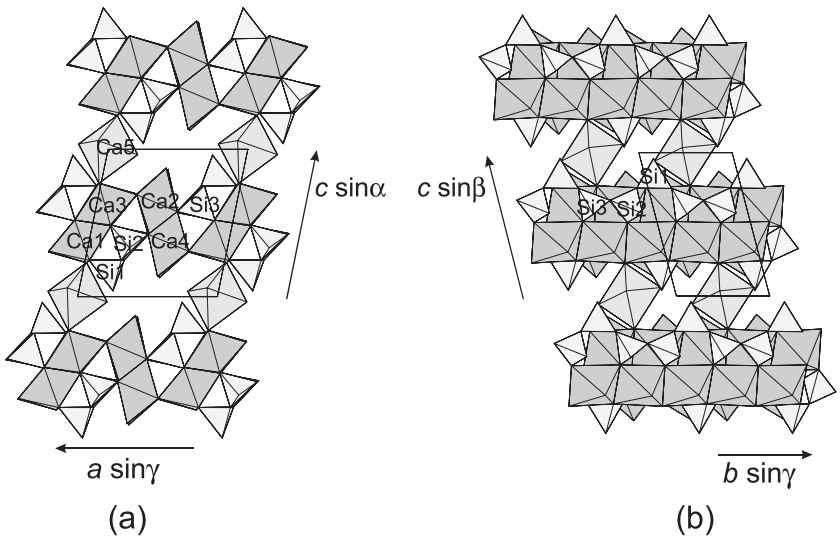

Fig. 2. Crystal structure of jennite, as seen along (a) [010] and (b) [100].

Table 5
Bond valence balance for jennite (v.u.)

	Ca1	Ca2	Ca3	Ca4	Ca5	Si1	Si2	Si3	Σ_{an}		Σ'_{an}
O1	0.355		0.375			0.883			1.613	O	1.800
O2		0.346	0.375	0.365					1.086	OH	0.947
O3		0.375		0.230			1.039		1.999	O	1.999
		0.355									
O4	0.328		0.346				0.793		1.710	O	1.710
	0.243										
O5						0.907	1.157		2.064	O	2.064
O6						0.932		1.039	1.971	O	1.971
O7				0.114			0.958	0.932	2.004	O	2.127
O8						1.039			1.039	O	1.962
O9		0.355		0.250				0.984	1.935	O	1.935
				0.346							
O10	0.294		0.264					1.011	1.833	O	1.833
			0.264								
O11	0.355	0.355		0.310					1.020	OH	0.880
O12	0.336		0.319		0.237*				0.892	OH	0.892
O13				0.271					0.271	H_2O	−0.064
O14		0.212							0.212	H_2O	0.131
W1					0.346*				0.346	H_2O	0.065
W2					0.346*				0.346	H_2O	−0.039
Σ_{cat}	1.912	1.999	1.942	1.887	1.856	3.761	3.946	3.966			

Parameters were taken from Ref. [24].
The anionic bond valence sums, corrected by taking into account the hydrogen bonds system, are reported in the last column. The asterisks (*) mean two equivalent bonds for the given anion.

more geometrically equivalent ways; different ways of stacking neighbouring layers allow the existence of a series of both disordered and ordered (polytypes) sequences.

The symmetry of the average structure points to an OD layer with monoclinic symmetry. The single OD layer, presented in Fig. 4, has translation vectors $\mathbf{b}_{ODL} = -\mathbf{b}$, $\mathbf{c}_{ODL} = -\mathbf{a} - 2\mathbf{c}$ ($b_{ODL} = 7.284$ Å, $c_{ODL} = 21.632$ Å), third basic vector $\mathbf{a}_0 = \mathbf{a}/2 + \mathbf{b}/4$ ($a_0 = 4.974$ Å, $\beta = 104.84°$), and layer group symmetry $P(1)2/m1$ (the symmetry is only approximately valid for two of the water molecules in octahedral coordination around Ca5). Each subsequent layer is obtained from the preceding one, in the arrangement of Fig. 4, through the partial operations $2_{1/2}$ (rotation by 180°, followed by translation $\mathbf{b}_{ODL}/4$), as well as $n_{1,2}$ (reflection in

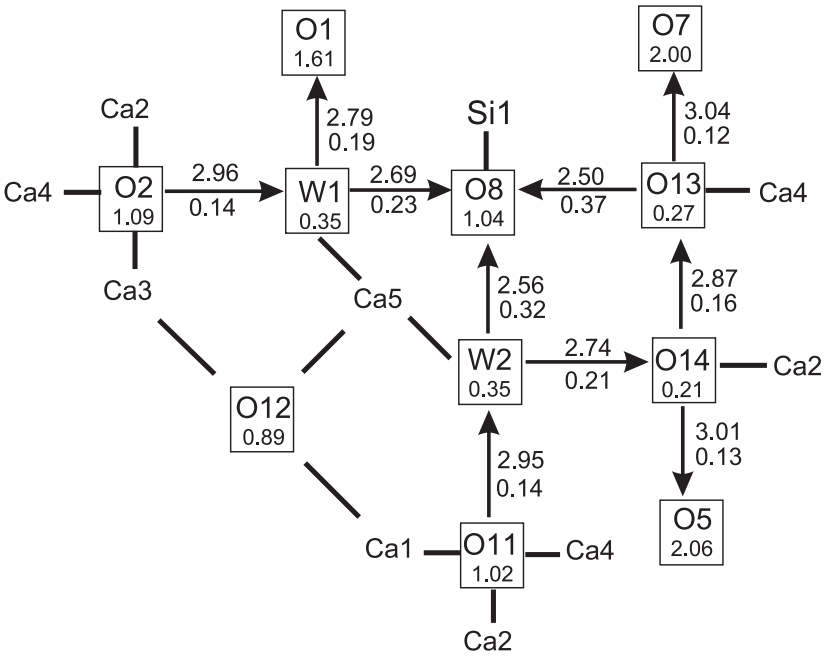

Fig. 3. Hydrogen bonding system in jennite. The O. . .O distance (Å) and the strength of the corresponding hydrogen bond (v.u.) are reported near to each arrow. The arrows point towards the acceptor atom in the hydrogen bond.

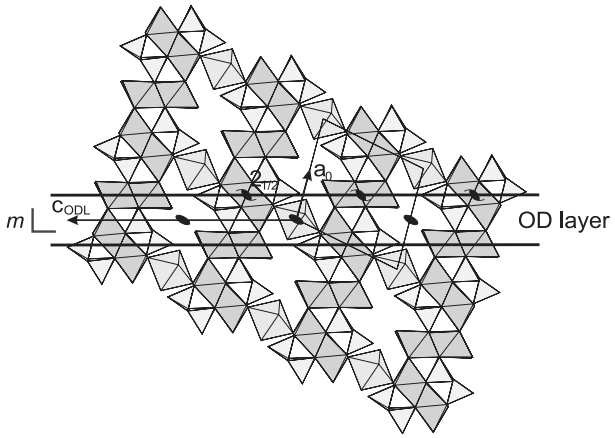

Fig. 4. OD layer in jennite. The symmetry elements of the layer (two fold axes along $\mathbf{b}_{ODL}$, and mirror plane m perpendicular to $\mathbf{b}_{ODL}$) are indicated, as well as the screw axes $2_{1/2}$, which relate adjacent OD layers. The unit cell of the triclinic jennite is outlined.

the horizontal plane, followed by translation $\mathbf{c}_{ODL}/2+ \mathbf{a}_0$). Subsequent layers may be connected also through the operations $2_{-1/2}$.

Pairs of layers built up with both operators ($2_{1/2}$ or $2_{-1/2}$) are geometrically equivalent. A whole family of OD structures may be obtained, characterised by different sequences of the operators. Their common symmetry properties are indicated by the symbol that presents the partial symmetry operations, which transform the layer into itself (first line) or into an adjacent layer (second line):

$$P \quad (1) \quad 2/m \quad 1$$

$$\{(1) \quad 2_{1/2}/n_{1,2} \quad 1\}$$

The parentheses in the first position of each line indicate that only $\mathbf{b}_{ODL}$ and $\mathbf{c}_{ODL}$ are translation vectors, whereas $\mathbf{a}_0$ is not a translation vector.

Two sequences correspond to the structures with maximum degree of order (MDO). In them, not only pairs, but also triples, quadruples, … n-tuples of subsequent OD layers are geometrically equivalent.

1) The sequence $2_{1/2}$, $2_{1/2}$, $2_{1/2}$, $2_{1/2}$, …, gives rise to MDO_1, triclinic, space group symmetry $P\bar{1}$, with:

$$\boldsymbol{a} = 2\boldsymbol{a}_0 + \boldsymbol{b}_{ODL}/2;\ \boldsymbol{b} = -\boldsymbol{b}_{ODL};$$
$$\boldsymbol{c} = -\boldsymbol{a}_0 + \boldsymbol{b}_{ODL}/4 - \boldsymbol{c}_{ODL}/2$$

and cell parameters just corresponding to those of the triclinic true cell of jennite (Table 1).
Obviously, the sequence $2_{-1/2}$, $2_{-1/2}$, $2_{-1/2}$, $2_{-1/2}$, …corresponds to the twin polytype (through the reflection in the plane normal to **b**).

2) The sequence $2_{1/2}$, $2_{-1/2}$, $2_{1/2}$, $2_{-1/2}$…gives rise to MDO_2, monoclinic, space group symmetry $P12/c1$, with:

$$\boldsymbol{a} = 2\boldsymbol{a}_0;\ \boldsymbol{b} = -\boldsymbol{b}_{ODL};\ \boldsymbol{c} = -2\boldsymbol{a}_0 - \boldsymbol{c}_{ODL}$$

and cell parameters: $a = 9.947$ Å, $b = 7.284$ Å, $c = 21.370$ Å, and $\beta = 101.90°$.

As a matter of fact, most crystals of natural jennite occur as substantially ordered MDO_1 triclinic polytype. In some cases, streaks parallel to **a*** for odd k values are evident, pointing to highly disordered sequences of the OD layers, which stack in the $\mathbf{a}_0$ direction. The streaking is more frequent in the synthetic specimens. No clear evidence has been so far obtained for the existence of largely ordered domains of the monoclinic MDO_2 polytype.

8. Relationships with metajennite

Jennite transforms to metajennite at 70–90 °C by losing four water molecules. A structural model for metajennite has been already sketched in Section 3. The results of our structural study of jennite now consent a more precise formulation of the structural arrangement of metajennite. The loss of the water molecules around the Ca5 calcium cations has severe consequences on the stability of the whole structure: not only is Ca5 no more properly coordinated, but also, the apical oxygen atom O8 of the bridging tetrahedron is no more an acceptor in the three strong hydrogen bonds with water molecules. The structure therefore reorganises itself in a shrinked phase by directly connecting successive composite tetrahedral–octahedral layers (the apical O8 oxygen atom of the bridging tetrahedron, which assures the connection, is now a hydroxyl group), thus consenting an appropriate coordination to Ca5 calcium cations.

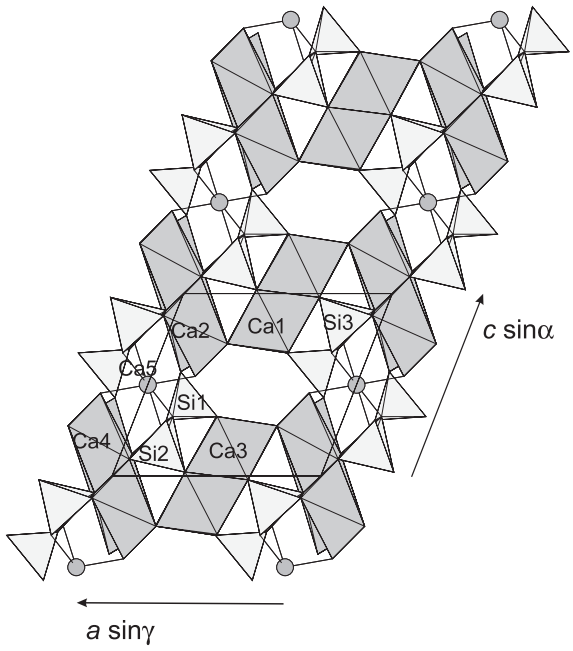

Fig. 5. Structural model of metajennite.

The structure of metajennite is presented in Fig. 5, where the Ca5 cation is tentatively located in a special position on the inversion centre, at 0, 0, 1/2, where it realises an acceptable octahedral coordination. The crystal chemical formula that corresponds to the discussed model, as well as to the indications in Ref. [2], is $Ca_9[Si_6O_{16}\ (OH)_2]\ (OH)_8.2H_2O$.

In contrast to jennite, no single crystal of metajennite has been found, and the structural model has not been refined. We are presently collecting powder diffraction data for carrying out a Rietveld refinement of the structure to define the actual position of the Ca5 cation, as well as of the water molecules indicated in the crystal chemical formula, and to definitely assess the whole crystal structure.

Metajennite too presents disorder with crystals exhibiting streaks parallel to **a*** for odd k values [1, 2]. As in the case of jennite, the disorder is a manifestation of its OD character. The single OD layer in metajennite is defined as that of jennite, obviously with reference to the actual parameters of metajennite; it presents the same layer group symmetry $P(1)2/m1$, and adjacent layers are related by $2_{1/2}$ or $2_{-1/2}$ operations. The constant application of the $2_{1/2}$ operation between succeeding layers gives rise to the triclinic form with the parameters given in Table 1 and structural model represented in Fig. 5.

Acknowledgements

This work has been supported by MIUR (Ministero dell'Università e della Ricerca Scientifica e Tecnologica) through grants to the projects COFIN 2001 'Structural complexity and mineral properties: microstructures, modularity, modulations' and FIRB RBAU011AKZ_004 'Properties and technological applications of minerals and their synthetic analogues'. The results described in this paper were presented in the 1st Prof. H F W Taylor memorial lecture, which was held during the 23rd Cement and Concrete Science meeting, 8–9th September 2003, University of Leeds.

References

[1] A.B. Carpenter, R.A. Chalmers, J.A. Gard, K. Speakman, H.F.W. Taylor, Jennite, a new mineral, Am. Mineral. 51 (1966) 56–74.
[2] J.A. Gard, H.F.W. Taylor, G. Cliff, G.W. Lorimer, A reexamination of jennite, Am. Mineral. 62 (1977) 365–368.
[3] S. Gross, The mineralogy of the Hatrurim formation, Israel, Bull. Geol. Surv. Israel 70 (1977) 1–80.
[4] A. Wittern, Mineralfundorte und ihre Minerale in Deutschland, E. Schweizerbart'sche Verlagsbuchhandlung, Science, Stuttgart, 2001.
[5] W. Schüller, Die Mineralien des Bellerberges bei Ettringen, Lapis 15 (5) (1990) 9–26.
[6] E. Passaglia, B. Turconi, Silicati e altri minerali di Montalto di Castro (Viterbo), Riv. Mineral. Ital. 4 (1982) 97–110.
[7] I. Kusachi, C. Henmi, K. Henmi, Afwillite and jennite from Fuka, Okayama Prefecture, Japan, Mineral. J. 14 (1989) 279–292.
[8] K.L. Von Bezing, R.D. Dixon, D. Pohl, G. Cavallo, The Kalahari manganese field: An update, Mineral. Rec. 22 (3) (1991) 279–302.
[9] Q.H. Abdul-Jaber, H. Khoury, Unusual mineralisation in the Maqarin Area (North Jordan) and the occurrence of some rare minerals in the marbles and the weathered rocks, Neues Jahrb. Geol. Paläontol. Abh. 208 (1998) 603–629.
[10] N. Hara, N. Inoue, Formation of jennite from fumed silica, Cem. Concr. Res. 10 (1980) 677–682.
[11] X. Cong, R.J. Kirkpatrick, ^{29}Si and ^{17}O NMR investigation of the structure of some crystalline calcium silicate hydrates, Adv. Cem. Based Mater. 3 (1996) 133–143.
[12] H.F.W. Taylor, Cement Chemistry, second ed., Thomas Telford, London, 1997.
[13] J.J. Chen, J.J. Thomas, H.F.W. Taylor, H.M. Jennings, Solubility and structure of calcium silicate hydrate, Cem. Concr. Res. 34 (2004) 1481–1488.
[14] D. Viehland, L.J. Yuan, Z. Xu, X. Cong, R.J. Kirkpatrick, Structural studies of jennite and 1.4 nm tobermorite: disordered layering along the [100] of jennite, J. Am. Ceram. Soc. 80 (12) (1997) 3021–3028.
[15] S. Komarneni, D.M. Roy, C.A. Fyfe, G.J. Kennedy, Naturally occurring 1.4nm tobermorite and synthetic jennite: Characterization by ^{27}Al and ^{29}Si MASNMR spectroscopy and cation exchange properties, Cem. Concr. Res. 17 (1987) 891–895.
[16] R.J. Kirkpatrick, J.L. Yarger, P.F. McMillan, P. Yu, X. Cong, Raman spectroscopy of C–S–H, tobermorite, and jennite, Adv. Cem. Based Mater. 5 (1997) 93–99.
[17] P. Yu, R.J. Kirkpatrick, B. Poe, P.F. McMillan, X. Cong, Structure of calcium silicate hydrate (C–S–H): Near-, mid-, and far-infrared spectroscopy, J. Am. Ceram. Soc. 82 (3) (1999) 742–748.
[18] H.F.W. Taylor, The calcium silicate hydrates, Proc. 5th Int. Symp. Chem. Cement, Tokyo, 1968 2.
[19] N.V. Belov, Crystal Chemistry of Large-Cation Silicates, Consultant Bureau Enterprises, New York, 1963.
[20] H. Sarp, D.R. Peacor, Jaffeite, a new hydrated calcium silicate from the Kombat mine, Namibia, Am. Mineral. 74 (1989) 1203–1206.
[21] N.A. Yamnova, K. Sarp, Y.K. Egorov-Tismenko, D.Y. Pushcharovskii, Crystal structure of jaffeite, Kristallografiya 38 (1993) 73–78.
[22] Z. Otwinowsky, W. Minor, Processing of X-ray diffraction data collected in oscillation mode, Methods Enzymol. 276A.
[23] G.M. Sheldrick, SHELXL-93. Program for the Refinement of Crystal Structures, Univ. Göttingen, Germany, 1997.
[24] N.E. Brese, M. O'Keeffe, Bond-valence parameters for solids, Acta Crystallogr. B47 (1991) 192–197.
[25] G. Ferraris, G. Ivaldi, Bond valence vs bond length in O···O hydrogen bonds, Acta Crystallogr. B44 (1988) 341–344.
[26] P. Yu, R.J. Kirkpatrick, Thermal dehydration of tobermorite and jennite, Concr. Sci. Eng. 1 (1999) 185–191.
[27] K. Dornberger Schiff, On the order–disorder (OD-structures), Acta Crystallogr. 9 (1956) 593–601.
[28] K. Dornberger Schiff, Grundzüge einer Theorie von OD—Strukturen aus Schichten, Abhandlungen der Deutschen Akademie der Wissenschaften zu Berlin, Klasse für Chemie, Geol. Biol. 3 (1964) 1–107.
[29] S. Ďurovič, Fundamentals of the OD theory, in: S. Merlino (Ed.), Modular Aspects of Minerals-EMU Notes in Mineralogy vol. 1, Eötvös Univ. Press, Budapest, 1997, pp. 29–54.
[30] G. Ferraris, E. Makovicky, S. Merlino, Crystallography of modular materials, IUCr Monographs in Crystallography, Oxford University Press, Oxford, 2004.